PHYSICAL REVIEW B **74**, 041301(R) (2006)

Anomalous in-plane magneto-optical anisotropy of self-assembled quantum dots

T. Kiessling,[1] A. V. Platonov,[2] G. V. Astakhov,[1,2,*] T. Slobodskyy,[1] S. Mahapatra,[1] W. Ossau,[1] G. Schmidt,[1] K. Brunner,[1] and L. W. Molenkamp[1]

[1]*Physikalisches Institut (EP3) der Universität Würzburg, 97074 Würzburg, Germany*

[2]*A. F. Ioffe Physico-Technical Institute, Russian Academy of Sciences, 194021 St. Petersburg, Russia*

(Received 31 March 2006; revised manuscript received 7 June 2006; published 10 July 2006)

We report on a complex nontrivial behavior of the optical anisotropy of quantum dots that is induced by a magnetic field in the plane of the sample. We find that the optical axis either rotates in the opposite direction to that of the magnetic field or remains fixed to a given crystalline direction. A theoretical analysis based on the exciton pseudospin Hamiltonian unambiguously demonstrates that these effects are induced by isotropic and anisotropic contributions to the heavy-hole Zeeman term, respectively. The latter is shown to be compensated by a built-in uniaxial anisotropy in a magnetic field B_C=0.4 T, resulting in an optical response typical for symmetric quantum dots.

DOI: 10.1103/PhysRevB.74.041301 PACS number(s): 78.67.Hc, 71.70.−d, 78.55.Et

Self-assembled semiconductor quantum dots (QDs) attract much fundamental and practical research interest, e.g., QDs have been proposed as optically controlled qubits.[1,2] An important aspect of QDs is the relationship between their symmetry and their optical properties. Many actual QDs, grown by molecular beam epitaxy, exhibit an elongated shape in the plane and a similar strain profile; their symmetry is reduced to C_{2v} or below. In this case the in-plane heavy-hole g factor is no longer isotropic.[3] Moreover, even in zero field the degeneracy of the radiative doublet is lifted due to the anisotropic exchange splitting.[4–6] Any of these issues will give rise to optical anisotropy, resulting in the linear polarization of the photoluminescence (PL).[3–7] In addition, the anisotropy of QDs can lead to optical polarization conversion in zero magnetic field.[8]

In this paper, we discuss the optical anisotropy of QDs in the presence of a magnetic field. Classically, the polarization axis of the luminescence of a given sample should be collinear with the direction of the magnetic field. This so-called Voigt effect implies that when rotating the sample over an angle α while keeping the direction of the magnetic field fixed, one observes a constant (in direction and amplitude) polarization for the luminescence. Mathematically one can express this behavior as following a zeroth-order spherical harmonic dependence on α. This situation changes drastically for low-dimensional heterostructures because of the complicated valence band structure. Kusrayev *et al.*[9] observed a second spherical harmonic component (i.e., π-periodic oscillations under sample rotation) in the polarization of emission from narrow quantum wells (QWs). This result was explained in terms of a large in-plane anisotropy of the heavy-hole g factor $g_{hh}^{xx}=-g_{hh}^{yy}$. Subsequently, this interpretation was substantiated using a microscopic theory.[10,11]

Here, we report the observation of a fourth harmonic in the magneto-optical anisotropy [i.e., $(\pi/2)$-periodic oscillations in the polarization of the emitted light under sample rotation] from CdSe/ZnSe self-assembled QDs. We demonstrate that this effect is quite general. Moreover, in contrast to earlier studies of in-plane magneto-optical anisotropies, we consider the contributions of the electron-hole exchange interaction, which have been ignored for QWs,[9,10] and are zero for charged QDs.[3] An anisotropic exchange splitting may lead to the occurrence of a compensating magnetic field B_C. When the externally applied field equals B_C, the amplitude of the second harmonic crosses zero, resulting in a highly symmetrical optical response of extremely anisotropic QDs.

In order to measure anisotropy we used the detection scheme presented in Fig. 1(a). The direction of the in-plane magnetic field is fixed, while the sample is rotated over an angle α. The degree of linear polarization is now defined as $\rho_\gamma(\alpha)=(I_\gamma-I_{\gamma+90°})/(I_\gamma+I_{\gamma+90°})$. Here the angle γ corresponds to the orientation of the detection frame with respect to the

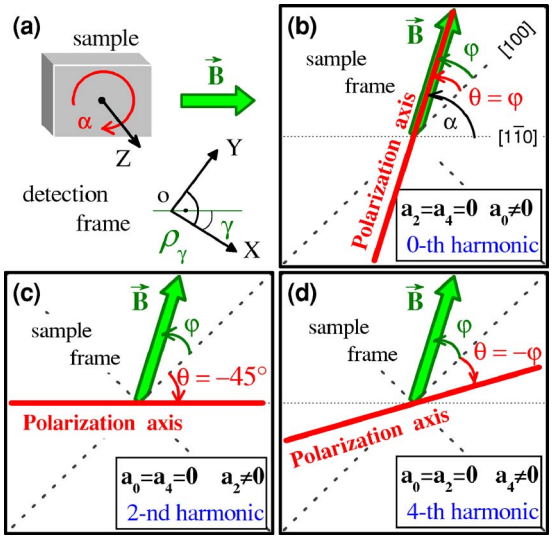

FIG. 1. (Color online) (a) Schematic layout of the angle-resolved experiments where α is the rotation angle of the sample. The detection frame ρ_γ is rotated by an angle γ (equal to 0° or 45°) with respect to the magnetic field **B**. (b)–(d) Different scenarios for magneto-optical anisotropy (shown in the sample frame). (b) The polarization axis follows the magnetic field and $\theta=\varphi$, leading to a zeroth harmonic in the angle scan. (c) The polarization axis is fixed (θ=const), resulting in a second harmonic in the angle scan. (d) The polarization axis rotates away from the magnetic field with $\theta=-\varphi$, leading to a fourth harmonic in the angle scan.

magnetic field and I_γ is the intensity of the PL polarized along the direction γ. Within an approximation of weak magnetic fields, a sample that has C_{2v} point symmetry in general may have only three spherical harmonic components[9] linking the polarization of the emission to the sample rotation angle α. Thus, one has for $\gamma=0°$ and $\gamma=45°$,

$$\rho_0(\alpha) = a_0 + a_2\cos 2\alpha + a_4\cos 4\alpha,$$

$$\rho_{45}(\alpha) = a_2\sin 2\alpha + a_4\sin 4\alpha, \qquad (1)$$

with a_0, a_2, and a_4 the amplitudes of the zeroth, second, and fourth harmonics, respectively. α is measured with respect to the $[1\bar{1}0]$ crystalline axis.

For an analysis of the various orientation effects it is more convenient to turn from the detection frame to the sample frame. Now the sample orientation is fixed and the magnetic field rotates by the same angle α but in the opposite direction [Figs. 1(b)–1(d)]. The orientation of the magnetic field in the spin Hamiltonian, which we discuss below, can be incorporated more conveniently using a basis along the [100], [010], and [001] crystalline axes. Therefore we introduce the angle φ between the magnetic field direction and the [100] axis, as $\varphi \equiv \alpha - 45°$. We then consider the orientation of the polarization axis described by an angle θ in the same [100] basis.

We are now in a position to discuss some limiting cases of Eq. (1). When the zeroth-order spherical harmonic dominates, $|a_0| \gg |a_2|, |a_4|$, the polarization axis of the emission coincides with the magnetic field direction for any orientation of the sample, $\theta(\varphi)=\varphi$ [Fig. 1(b)]. For a dominantly second harmonic response, $|a_2| \gg |a_0|, |a_4|$, the polarization axis is fixed to a distinct sample direction and does not depend on the magnetic field orientation. In our experiments, the fixed polarization axis is $[1\bar{1}0]$ and $\theta(\varphi)=-45°$ [Fig. 1(c)]. The most interesting behavior is observed for the fourth harmonic $|a_4| \gg |a_0|, |a_2|$, when the polarization $\rho_\gamma(\alpha)$ in the detection frame changes twice as fast as any polarization linked to the sample frame. This implies that the polarization axis turns in the opposite direction to that of the magnetic field, and $\theta(\varphi)=-\varphi$ [Fig. 1(d)]. In other words, it is collinear with the magnetic field when $\mathbf{B}\|[100],[010]$ and perpendicular to the magnetic field when $\mathbf{B}\|[110],[1\bar{1}0]$.

We studied the magneto-optical anisotropy of CdSe QDs in a ZnSe host. The samples were fabricated on (001) GaAs substrates using molecular beam epitaxy and self-assembly after depositing one monolayer of CdSe on a 50-nm-thick ZnSe layer. The QDs were then capped by 25 nm of ZnSe (for details of growth and characterization see Refs. 12 and 8). A typical PL spectrum, obtained at a temperature $T=1.6$ K, is shown in Fig. 2(a). For optical excitation at 2.76 eV we used a stilbene dye laser pumped by the uv lines of an Ar-ion laser. From systematic studies on the energetic structure of the QDs,[13] we know that excitation into the ZnSe barrier, where uncoupled electron-hole pairs are created, results mainly in the formation of charged excitons in the QDs. In order to form neutral excitons the excitation is kept below the ZnSe barrier. The polarization was then detected on the high-energy side of the PL band (2.68 eV) where the contribution of neutral excitons dominates over that from charged trions. For detection of the linear polarization we applied a standard technique using a photoelastic modulator.[8] The angle scans were performed with the samples mounted on a rotating holder controlled by a stepping motor with an accuracy better than1°. Magnetic fields up to 4 T were applied in the sample plane (Voigt geometry); optical excitation was done using a depolarized laser beam.

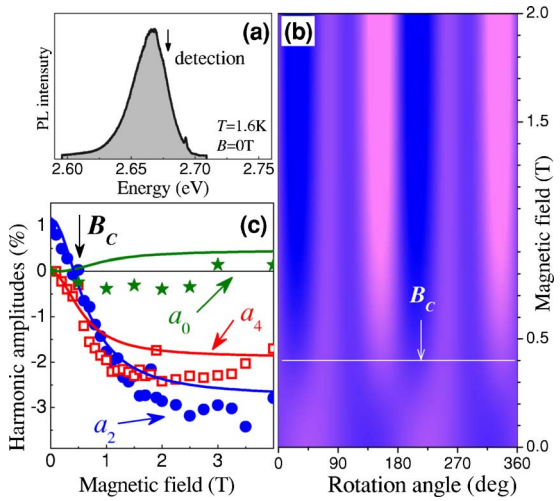

FIG. 2. (Color online) (a) PL emission spectrum of the CdSe/ZnSe QD sample. (b) Three-dimensional 3D plot of the linear polarization $\rho_{45}(\alpha,B)$ as function of the rotation angle α and magnetic inductance B. Light (red) and dark (blue) areas correspond to positive and negative values of $\rho_{45}(\alpha,B)$, respectively. (c) Amplitudes of the zeroth (a_0), second (a_2), and fourth (a_4) spherical harmonics vs B. The symbols are experimental data and the solid lines result from calculations. The arrows in (b) and (c) indicate the compensating field B_C where the linear polarization is $(\pi/2)$-periodic ($a_2=0$).

The result of angle scans of ρ_{45} for various magnetic field strengths is shown in Fig. 2(b). In zero magnetic field the linear polarization is π periodic [see also Fig. 3(a)]. This demonstrates the low (C_{2v}) symmetry of the QDs resulting in a finite value of a_2 in Eq. (1). One can regard this measurement as reflecting the "built-in" linear polarization of the array of dots. For high magnetic fields a_2 changes sign and an additional fourth harmonic signal appears [see also Fig. 3(c)]. At an intermediate magnetic field $B_C \approx 0.4$ T the second harmonic crosses zero, while the fourth harmonic remains finite [see also Fig. 3(b)]. The resulting $(\pi/2)$-periodic optical response corresponds to the higher (D_{2d}) symmetry expected for symmetric QDs. This observation clearly demonstrates that the in-plane optical anisotropy of QDs can be compensated by in-plane Zeeman terms. We also find that the zeroth harmonic signal is weak. This is clearly seen, e.g., for the ρ_0 angle scan in Fig. 3(d) which was taken for $B=4$ T, where the field-induced alignment is saturated.

We now model our observations using a pseudospin formalism.[10,14] We denote by $|+Sp\rangle$ and $|-Sp\rangle$ the wave functions of an electron (p=el) or heavy-hole (p=hh) with pseudospin projection $\pm S$ along the z direction. We define a pseudospin Hamiltonian in matrix form as

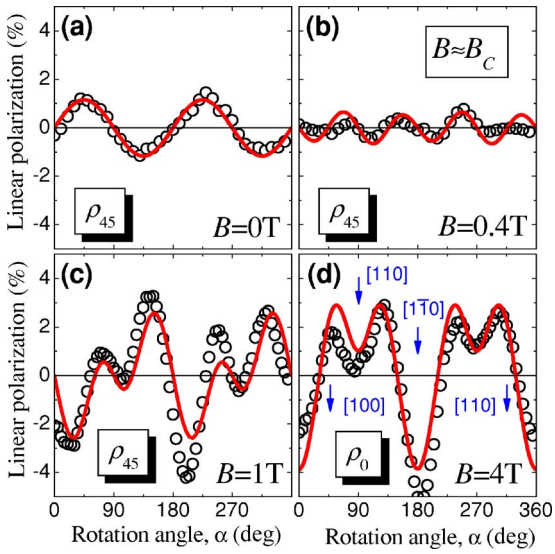

FIG. 3. (Color online) Angle scans of the linear polarization of the luminescence. The symbols are experimental data; solid lines represent calculations based on the Hamiltonian of Eq. (7). (a) Built-in linear polarization (B=0 T). (b) A highly symmetrical optical response [i.e., $(\pi/2)$-periodic] appears at a compensating field $B_c \approx 0.4$ T. (c) Angle scan in a magnetic field B=1 T exceeding B_C. (d) Angle scan in the saturation regime, B=4 T. The detection frame ρ_γ in (a)–(c) is rotated by an angle γ=45°; in (d) γ=0°. The arrows indicate the points where the orientation of the magnetic field aligns with high-symmetry directions in the sample frame.

$$\mathcal{H}_p = \frac{\delta_p}{2}(\sigma_x \cos\theta_p + \sigma_y \sin\theta_p), \tag{2}$$

where σ_x and σ_y are the Pauli matrices. This Hamiltonian has eigenfunctions $\Psi_p^{\pm 1} \propto |+Sp\rangle \pm e^{i\theta_p}|-Sp\rangle$. The optical matrix elements for a transition between electron and heavy-hole bands are $\langle \pm\frac{1}{2}\mathrm{el}|\hat{P}|\pm\frac{3}{2}\mathrm{hh}\rangle = \mp e_\pm$,[6] where $\hat{P}$ is the dipole momentum operator. We define $e_\pm = (e_x \pm i e_y)/\sqrt{2}$ where $e_x \| [100]$ and $e_y \| [010]$ are unit vectors. We thus find for the optical matrix elements for the four possible optical transitions

$$\langle \Psi_{el}^{\eta}|\hat{P}|\Psi_{hh}^{\mu}\rangle \propto -e_+ + \eta\mu e^{i(\theta_{hh}-\theta_{el})}e_-. \tag{3}$$

These matrix elements thus predict a linear polarization with an axis that is rotated over an angle $\theta = \frac{1}{2}(\theta_{hh} - \theta_{el})$ from [100] when $\eta = -\mu$ $(\eta, \mu = \pm 1)$, and rotated over $\theta = \frac{1}{2}(\theta_{hh} - \theta_{el}) + 90°$ when $\eta = \mu$.

For an electron in an external magnetic field B, we can write the Zeeman Hamiltonian as

$$\mathcal{H}_{el} = \frac{1}{2} g_{el}^{\perp} \mu_B (\sigma_x B \cos\varphi + \sigma_y B \sin\varphi), \tag{4}$$

where $g_{el}^{\perp}$ is the electron g factor, yielding directly $\theta_{el} = \varphi$. For D_{2d} symmetry, the interaction of holes with an in-plane magnetic field B can be described by[15]

$$\mathcal{H}_{hh} = q_1 g_0 \mu_B (J_x^3 B \cos\varphi + J_y^3 B \sin\varphi), \tag{5}$$

where q_1 is a constant. It suffices to note that the parts of the matrices J_x^3 and J_y^3 related to the angular momentum of heavy holes behave as $\frac{3}{4}\sigma_x$ and $-\frac{3}{4}\sigma_y$, respectively.[6] On comparing with Eq. (2) this implies $\theta_{hh} = -\varphi$ for the eigenstate, yielding [cf. Eq. (3) and the text thereafter] a rotation over an angle $\theta = -\varphi$ or $\theta = -\varphi + 90°$ for the polarization of the luminescence. In accordance with Fig. 1(d) this corresponds to the fourth spherical harmonic.

The second harmonic may appear for structures with C_{2v} symmetry or below. In this case there is a correction to the magnetic interaction, given by[15]

$$\mathcal{H}'_{hh} = q_2 g_0 \mu_B (J_x^3 B \sin\varphi + J_y^3 B \cos\varphi), \tag{6}$$

where q_2 is C_{2v} invariant. From this correction one finds $\theta_{hh} = \varphi - 90°$, leading to a rotation of the luminescence polarization over $\theta = \pm 45°$, which implies [Fig. 1(c)] a response following a second spherical harmonic.

For a quantitative analysis a more detailed approach is required which we provide below. The essential experimental data are summarized in Fig. 2(c), where we plot the amplitudes of the spherical harmonic, i.e., the coefficients a_0, a_2, and a_4, extracted from the fits of the experimental data on $\rho_\gamma(\alpha)$ using Eq. (1) vs magnetic field (symbols).

In QDs, the electron-hole exchange interaction is significant and a corresponding term $\mathcal{H}_{ex}$ must be taken into account,[16] resulting in an exchange splitting δ_0 between the $|\pm 1\rangle$ and $|\pm 2\rangle$ exciton states. Moreover, $\mathcal{H}_{ex}$ leads to a splitting $\delta_2 < \delta_0$ of the nonradiative exciton states. When the symmetry is lowered to C_{2v}, an anisotropic exchange term[6,17] $\mathcal{H}'_{ex}$ appears and results in an additional splitting δ_1 of the radiative doublet.

In the basis of the exciton states $\Phi_{1,2} = |\pm 1\rangle$ and $\Phi_{3,4} = |\pm 2\rangle$, the final spin Hamiltonian $\mathcal{H} = \mathcal{H}_{el} + \mathcal{H}_{hh} + \mathcal{H}'_{hh} + \mathcal{H}_{ex} + \mathcal{H}'_{ex}$ is given by[6,17]

$$\mathcal{H} = \frac{1}{2}\begin{pmatrix} \delta_0 & -i\delta_1 & \delta_{el} & \delta_{hh} \\ i\delta_1 & \delta_0 & \delta_{hh}^* & \delta_{el}^* \\ \delta_{el}^* & \delta_{hh} & -\delta_0 & \delta_2 \\ \delta_{hh}^* & \delta_{el} & \delta_2 & -\delta_0 \end{pmatrix}. \tag{7}$$

Here, $\delta_{el} = \mu_B g_{el}^{\perp} B_+$ and $\delta_{hh} = \mu_B (g_{hh}^{\mathrm{i}} B_+ + i g_{hh}^{\mathrm{a}} B_-)$ are in-plane Zeeman terms; $g_{hh}^{\mathrm{i}} = \frac{3}{2} g_0 q_1$ and $g_{hh}^{\mathrm{a}} = \frac{3}{2} g_0 q_2$ are the isotropic and anisotropic contributions to the heavy-hole g factor. $B_\pm = B e^{\pm i\varphi}$ are effective magnetic fields. Analytical solutions for the normalized eigenfunctions $\Psi_j = \Sigma V_{nj} \Phi_n$ and the energy eigenvalues E_j of Hamiltonian (7) can be found in the high-magnetic-field limit $(|\delta_{hh}|, |\delta_{el}| \gg |\delta_0|, |\delta_1|, |\delta_2|)$,as follows:

$$V = \frac{1}{2}\begin{pmatrix} 1 & 1 & 1 & 1 \\ e^{2i\theta} & -e^{2i\theta} & -e^{2i\theta} & e^{2i\theta} \\ -e^{-i\theta_{el}} & e^{-i\theta_{el}} & -e^{-i\theta_{el}} & e^{-i\theta_{el}} \\ -e^{i\theta_{hh}} & -e^{i\theta_{hh}} & e^{i\theta_{hh}} & e^{i\theta_{hh}} \end{pmatrix},$$

$$E_{1,4} = \mp|\delta_{el}| \mp |\delta_{hh}|, \quad E_{2,3} = \pm|\delta_{el}| \mp |\delta_{hh}|, \tag{8}$$

where $e^{i\theta_{el}} = \delta_{el}/|\delta_{el}|$, $e^{i\theta_{hh}} = \delta_{hh}^*/|\delta_{hh}|$, and $e^{2i\theta} = e^{i(\theta_{hh}-\theta_{el})}$ have the same meaning as in Eq. (3). Equations (8) clearly show the same trends expected from the qualitative analysis presented above [Eqs. (2)–(6)]. For a given finite magnetic field, solutions for E_j and Ψ_j can easily be calculated numerically.

Using the solutions to Hamiltonian (7) we may obtain the intensity and polarization of the luminescence. Since only the $\Phi_{1,2}=|\pm 1\rangle$ excitons are optically active, the optical matrix element in an arbitrary direction $\mathbf{e}$ for eigenfunction Ψ_j can be written as $M_j(\mathbf{e})=-V_{1j}e_+ + V_{2j}e_-$.[17] We then can calculate the intensity of the luminescence linearly polarized along an axis rotated by an angle ξ with respect to the [100] crystalline axis as $I_{j,(\xi)}=|M_j(\mathbf{e}||\xi)|^2$.

The polarization of the PL from an ensemble of QDs must be averaged over the thermal population of exciton states, and can in the sample frame be expressed as

$$\rho'_{(\xi)} = K\frac{\sum_j P_j(I_{j,(\xi)} - I_{j,(\xi+90^\circ)})}{\sum_j P_j(I_{j,(\xi)} + I_{j,(\xi+90^\circ)})}, \tag{9}$$

where $P_j \propto e^{-E_j/k_BT}$ is the Boltzmann factor. K is a scaling factor that corrects for spin relaxation, and basically determines the saturation level of the polarization at high magnetic fields.

Using this approach, we have calculated the linear polarizations $\rho'_{(100)}$ and $\rho'_{(1\bar{1}0)}$ in the sample frame using Eq. (9). From this, we found the polarizations $\rho_0(\alpha)=\rho'_{(1\bar{1}0)}\cos 2\alpha + \rho'_{(100)}\sin 2\alpha$ and $\rho_{45}(\alpha)=\rho'_{(1\bar{1}0)}\sin 2\alpha - \rho'_{(100)}\cos 2\alpha$. We were able to reproduce all experimental data using a unique set of parameters for given excitation power and excitation energy. The calculations were done taking a bath temperature $T=1.6$ K and a coefficient $K=0.04$. From the best fits we found exchange energies $\delta_0=2.9$ meV, $\delta_2=0.1$ meV, $\delta_1=0.2$ meV and g factors $g_e^{\perp}=1.1$, $g_{hh}^i=-0.5$, $g_{hh}^a=0.6$.

Exemplary results of the calculations are the solid lines in Fig. 3, which follow the experimental data very closely. For a large number of similar fits we have evaluated the harmonic amplitudes (a_0, a_2, and a_4) using Fourier transformation. The results as a function of magnetic field are plotted as solid lines Fig. 2(c). From this plot we find a compensating field B_C of 0.42 T, which coincides with the experimental value.

Finally, we discuss contributions arising from the mixing of heavy (hh) and light (lh) holes. First, it modifies the coefficients q_1 and q_2,[15] which are dealed with in Eqs. (5)–(7). Second, it directly affects the polarization of the optical transitions as the hole wave function is now written in the form $|\pm\frac{3}{2}\mathrm{hh}\rangle + \beta|\mp\frac{1}{2}\mathrm{lh}\rangle$. In analogy with Eqs. (2)–(6) one can show that the light hole gives rise to a zeroth harmonic component instead of a fourth one. In the samples studied in our work the zeroth harmonic appeared to be weak, and therefore the contribution of the light-hole band to the exciton eigenfunctions is neglected. This may explain some discrepancy of the calculated a_0 from the data in Fig. 2(c). We also note that the heavy-light hole mixing gives rise to a linear dichroism of the QDs, $\tilde{\rho}$, which is independent of temperature and magnetic field.[10,11] For $\rho \ll 1$ this contribution is additive to Eq. (9) and thus can be considered phenomenologically. However, based on the present experimental data we cannot distinguish between the contributions of the built-in linear polarization arising from the anisotropic exchange splitting δ_1 and the linear dichroism. In general, we are able to fit them with any reasonable value of $\tilde{\rho}$, and for the sake of simplicity the presented calculations are obtained with $\tilde{\rho}=0$.

Summarizing, we have observed anomalous behavior of the in-plane magneto-optic anisotropy in CdSe/ZnSe QDs, in that the second and fourth spherical harmonics of the response dominate over the classical zeroth-order response. We show the existence of a compensating magnetic field, leading to a symmetry enhancement of the QD optical response. All of these findings could be modeled using a pseudospin Hamiltonian approach. The physics responsible for our findings is not limited to QDs and can be applied to other heterostructures of the same symmetry where the heavy-hole exciton is the ground state.

This work was supported by the Deutsche Forschungsgemeinschaft (SFB 410) and RFBR.

*Email address: astakhov@physik.uni-wuerzburg.de

[1] D. Loss and D. P. DiVincenzo, Phys. Rev. A **57**, 120 (1998).
[2] A. Shabaev, A. L. Efros, D. Gammon, and I. A. Merkulov, Phys. Rev. B **68**, 201305 (2003).
[3] A. V. Koudiniov, I. A. Akimov, Y. G. Kusrayev, and F. Henneberger, Phys. Rev. B **70**, 241305(R) (2004).
[4] D. Gammon, E. S. Snow, B. V. Shanabrook, D. S. Katzer, and D. Park, Phys. Rev. Lett. **76**, 3005 (1996).
[5] M. Bayer, A. Kuther, A. Forchel, A. Gorbunov, V. B. Timofeev, F. Schäfer, J. P. Reithmaier, T. L. Reinecke, and S. N. Walck, Phys. Rev. Lett. **82**, 1748 (1999).
[6] E. L. Ivchenko, *Optical Spectroscopy of Semiconductor Nanostructures* (Alpha Science, Harrow, U.K., 2005).
[7] D. N. Krizhanovskii, A. Ebbens, A. I. Tartakovskii, E. Pulizzi, T. Wright, M. S. Skolnick, and M. Hopkinson, Phys. Rev. B **72**, 161312 (2005).
[8] G. V. Astakhov, T. Kiessling, A. V. Platonov, T. Slobodskyy, S. Mahapatra, W. Ossau, G. Schmidt, K. Brunner, and L. W. Molenkamp, Phys. Rev. Lett. **96**, 027402 (2006).
[9] Yu. G. Kusrayev, A. V. Koudinov, I. G. Aksyanov, B. P. Zakharchenya, T. Wojtowicz, G. Karczewski, and J. Kossut, Phys. Rev. Lett. **82**, 3176 (1999).
[10] Y. G. Semenov and S. M. Ryabchenko, Phys. Rev. B **68**, 045322 (2003).
[11] A. V. Koudinov, N. S. Averkiev, Yu. G. Kusrayev, B. R. Namozov, B. P. Zakharchenya, D. Wolverson, J. J. Davies, T. Wojtowicz, G. Karczewski, and J. Kossut, cond-mat/0601204 (unpublished).
[12] S. Mahapatra, C. Schumacher, T. Kiessling, G. V. Astakhov, U. Bass, W. Ossau, J. Geurts, and K. Brunner, Acta Phys. Pol. A **108**, 769 (2005).
[13] A. V. Platonov *et al.*, Phys. Status Solidi C **3**, 924 (2006).
[14] I. A. Merkulov and K. V. Kavokin, Phys. Rev. B **52**, 1751 (1995).
[15] G. E. Pikus and F. G. Pikus, Solid State Commun. **89**, 319 (1994).
[16] M. Bayer *et al.*, Phys. Rev. B **65**, 195315 (2002).
[17] G. E. Pikus and F. G. Pikus, J. Lumin. **54**, 279 (1992).